Supplementary Information for

Angle Robust Plasmonic Color Printing of Deep Subwavelength Nanopixelated Sodium Metasurfaces

Jie Liang[1#], Yurui Qu[2#], Huizhen Zhang[1], Yuhan Yang[1], Yang Wang[1], Yuchen Zhang[1], Zhenda Lu[1], Shining Zhu[1], Lin Zhou[1*]

[1] National Laboratory of Solid State Microstructures, College of Engineering and Applied Sciences, Jiangsu Key Laboratory of Artificial Functional Materials, Key Laboratory of Intelligent Optical Sensing and Manipulation, Ministry of Education, Nanjing University, Nanjing, P. R. China, 210093

[2] School of Information Science and Technology, ShanghaiTech University, Shanghai, P. R. China, 201210

* Corresponding authors: linzhou@nju.edu.cn

[#] These authors contributed equally to this work.

Supplementary Note

Note S1 Fabrication of quartz template with nanoholes:

The proposed sodium nanostructures were fabricated on a quartz substrate by using a thermal-assisted spin-coating process. Supplementary Fig. 1 shows a schematic of the key fabrication process steps for the angular insensitive plasmonic color palettes. Firstly, a 30 nm-thick silver (Ag) thin film was deposited onto the clear quartz (thickness about 0.5 mm) at a rate of 0.2 nm/s as a conductive layer employing physical vapour deposition (Gatan 682). The pre-designed nanostructures were then drilled on the quartz substrate via focused-ion-beam (FIB) milling (Dual-beam FIB 235, FEI Strata) at an acceleration voltage of 30 kV and a beam current of 250 pA. Subsequently, the Ag film was dissolved in HNO_3 and the quartz with nanostructures was ultrasonically cleaned in deionized (DI) water. After annealing in a muffle furnace at 700°C for 20 minutes, the quartz substrate was then subjected to ion beam etching (IBE) to remove gallium.

Note S2 Spin-coating process:

We took advantage of the low melting point of sodium (97.7 °C) to fabricate arrays of sodium nanorods on nanopore-patterned quartz using a thermo-assisted spin-coating process in an inert-atmosphere-equipped glove box. Once the liquid sodium droplet (~ 120 °C) were dropped freely from a relatively high height and then touches in nearby the center of the high-speed rotated quartz surface (6000 r/min), the liquid sodium droplet were rushed into the nanoholes of quartz under the interplay of the pronounced vertical impulse and strong centrifugal forces of the rotating quartz, forming a smooth nanorod surface by fast liquid metal solidification, and finally was packaged with epoxy.

Note S3 Optical measurements:

The reflection spectra and the optical microscope micrographs as a function of the incident angle were measured through an angle-resolved micro-spectroscopy system (ARM available from ideaoptics, China). Other common bright field optical images

were acquired with an optical microscope (Nikon, LV100ND) with×10 (0.3 NA) and ×20 (0.45 NA) air objectives at Kohler illumination, using a DS-Fi2 Microscope Camera (CCD). Most samples are measured from 0 ~ 30° incident light to obtain the angle-resolved reflectance using the ×100 objective (0.9 NA) with good optical signal up to 60°. Note that larger angle (> 60°) dependent spectra were tried as well in our lab but were unsuccessful due to the limited numerical aperture and inherently poor signals. We consider that the incident light cannot cover the plasmonic structure color pattern completely due to the deviation of the internal optical path of the instrument for large oblique angle incidence, which leads to the deterioration of the collected optical signals. The dark field optical image and scattering spectra were measured by the microscope (Axio Imager.A2m, Zeiss), with an objective lens (×50/0.8 NA, EC Epiplan-NEOFLUAR, Zeiss). The Scattering Spectrum was recorded by a Grating Spectrometer (Kymera 193i-A, Andor) and a CCD (iKon-M, Andor).

Note S4 Sodium filling morphology characterization:

To obtain the microscopic filling profile of the sodium metals inside the templated holes, we also conducted the vertical cutting procedure with FIB (ThermoFisher, Helios G4 CX) with a vacuum transfer chamber to protect the Na nanorods arrays sample from oxidation during transferring it from argon glove box to FIB system.

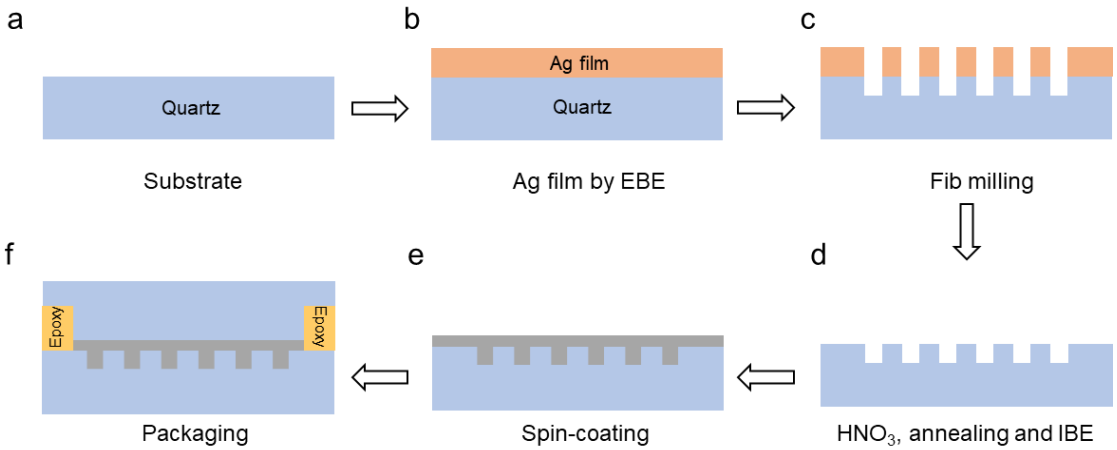

Supplementary Fig. S1. The fabrication process for designed sodium nanostructures.

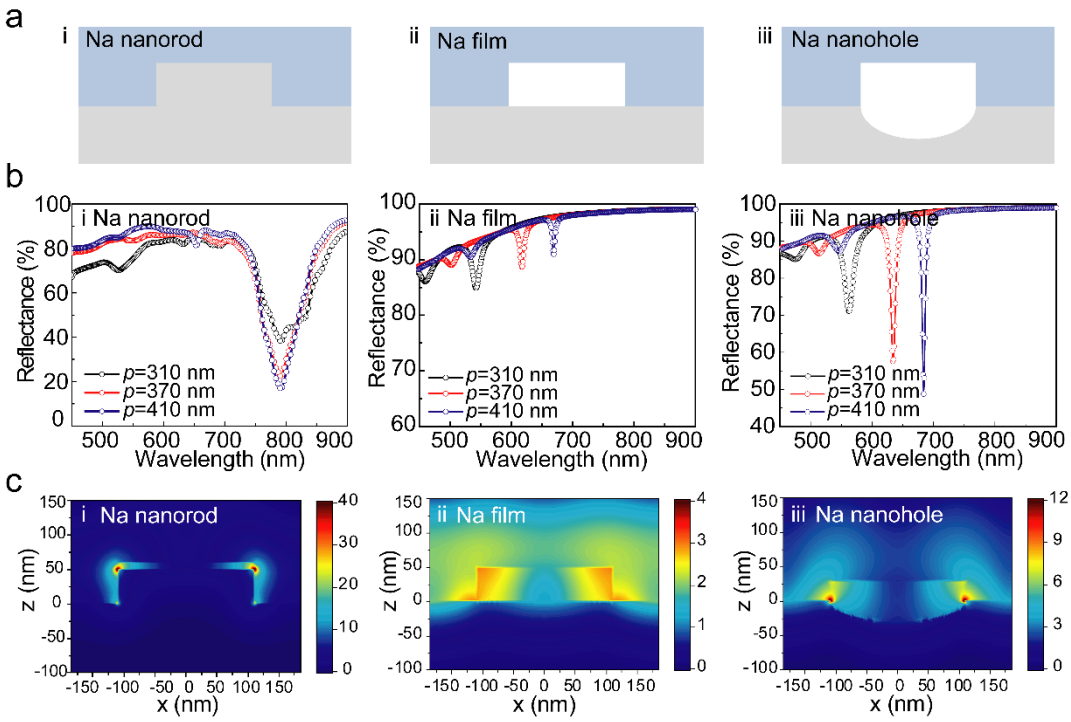

Supplementary Fig. S2. (a) The three different structure configurations schematics: Na nanorod (i), Na film (ii) and Na nanohole (iii). (b) The period-varied simulation reflectance spectra of three different configurations of nanostructure with diameter (*d*) 220 nm, height (*h*) 50 nm. (c) The electric field distributions of the three different structure configurations.

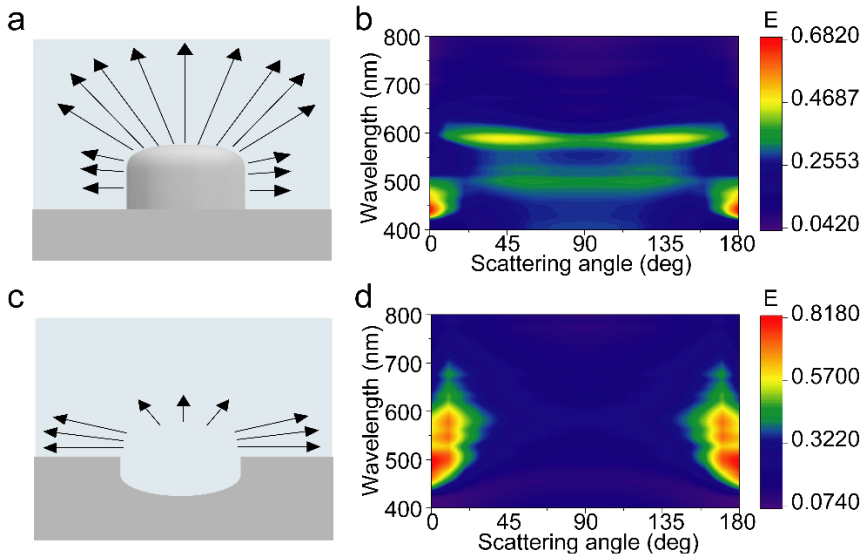

Supplementary Fig. S3. (a) The scattering schematic of the nanorod structure. (b) The simulation result of the electric field intensity in a semicircle of 90 nm around the single nanorod structure (d=120 nm h=30 nm) in (a) illuminated with TM polarized light. (c) The scattering schematic of the nanohole structure. (d) The simulation result of the electric field intensity in a semicircle of 90 nm around the single nanohole structure (d=120 nm h=30 nm) in (c) illuminated with TM polarized light.

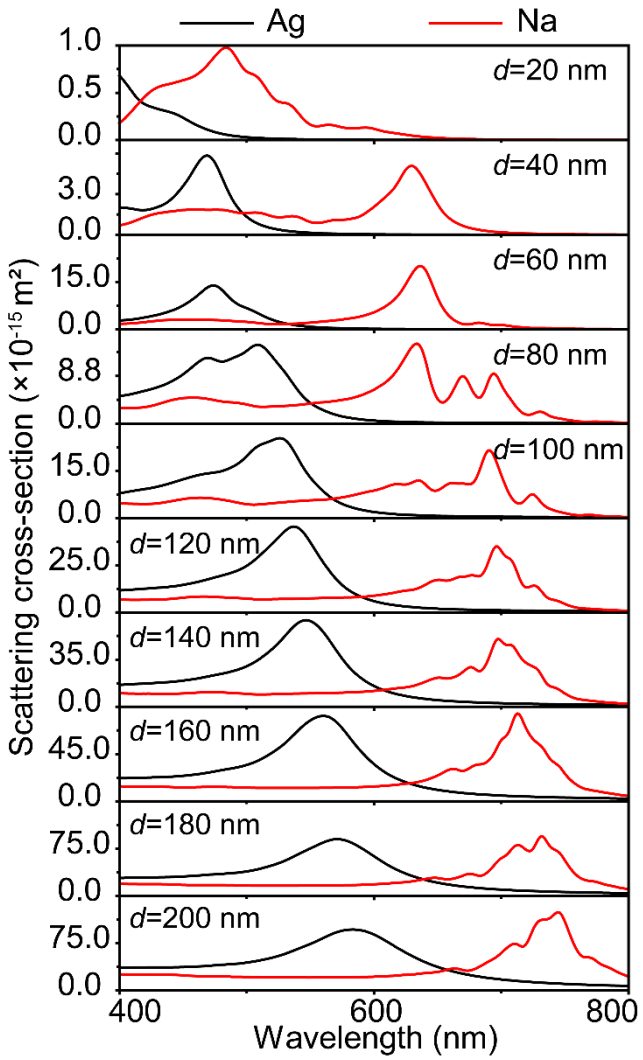

Supplementary Fig. S4. Scattering cross section comparison of Na and Ag nanorods with different diameters, showing the broader LSPR wavelength range of Na nanorods than that of Ag nanorods for the same diameter range.

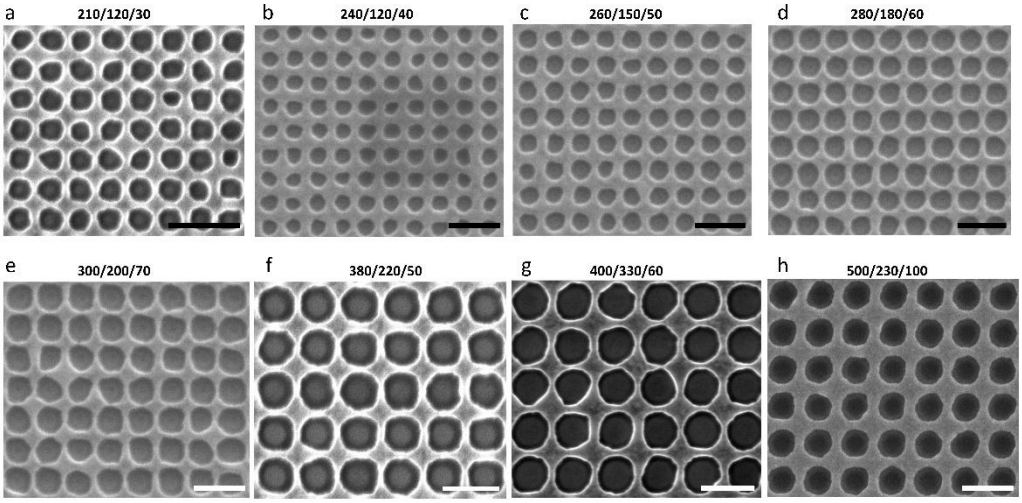

Supplementary Fig. S5. SEM images of the quartz substrates with nanoholes fabricated by FIB. The unit of *p*/*d*/*h* is nm. The scale bar is 500 nm.

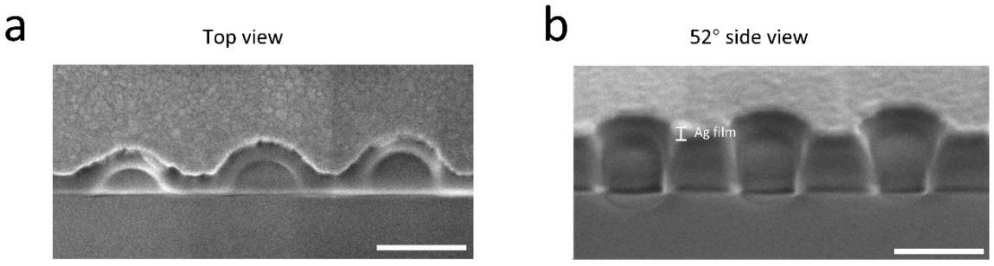

Supplementary Fig. S6. Top-view (a) and side-view (b) SEM images of the quartz substrates with a thin Ag film after FIB process. The cross-sectional view of the nanostructures in quartz shows that the structure has a cylindrical-like profile. The edges of the cylinder are slightly inclined due to the collimation problem of ion beam etching. The scale bar is 500 nm.

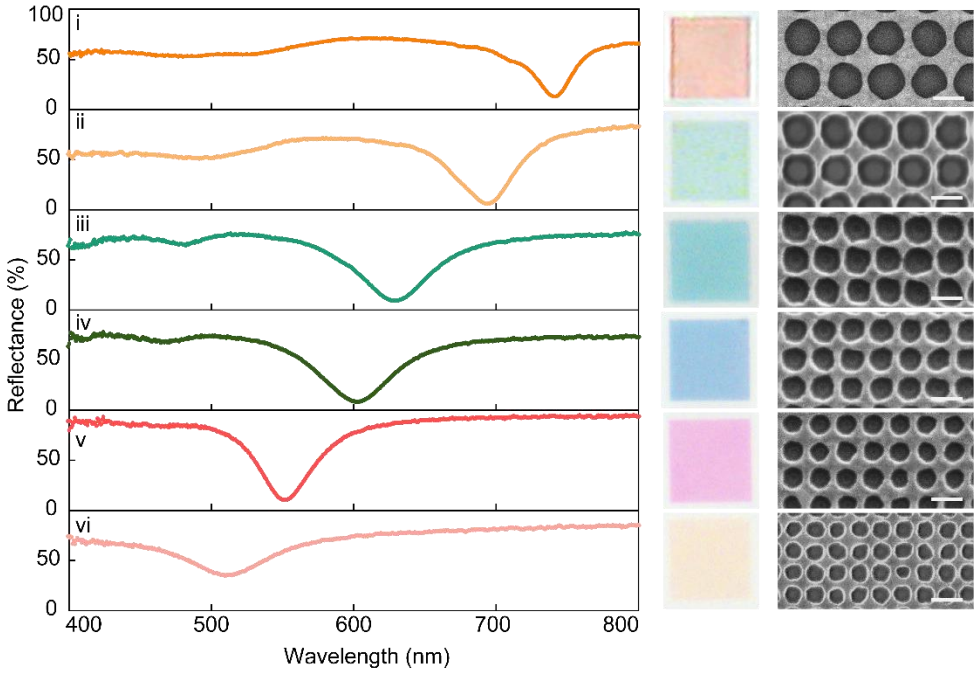

Supplementary Fig. S7. Experimental reflectance spectra of different sodium nanorods arrays under unpolarized incident light at 0°. The insets represent the unit cell period (p)), rod diameter (d) and height (h) of the nanorod: (i) p = 410 nm, d = 340 nm, h = 50 nm, (ii) p = 380 nm, d = 300 nm, h = 50 nm, (iii) p = 300 nm, d = 230 nm, h = 70 nm, (iv) p = 280 nm, d = 200 nm, h = 60 nm, (v) p = 260 nm, d = 150 nm, h = 40 nm, (vi) p = 210 nm, d = 120 nm, h = 30 nm, respectively. The corresponding optical and SEM images of the samples are on the right. The scale bar is 300 nm.

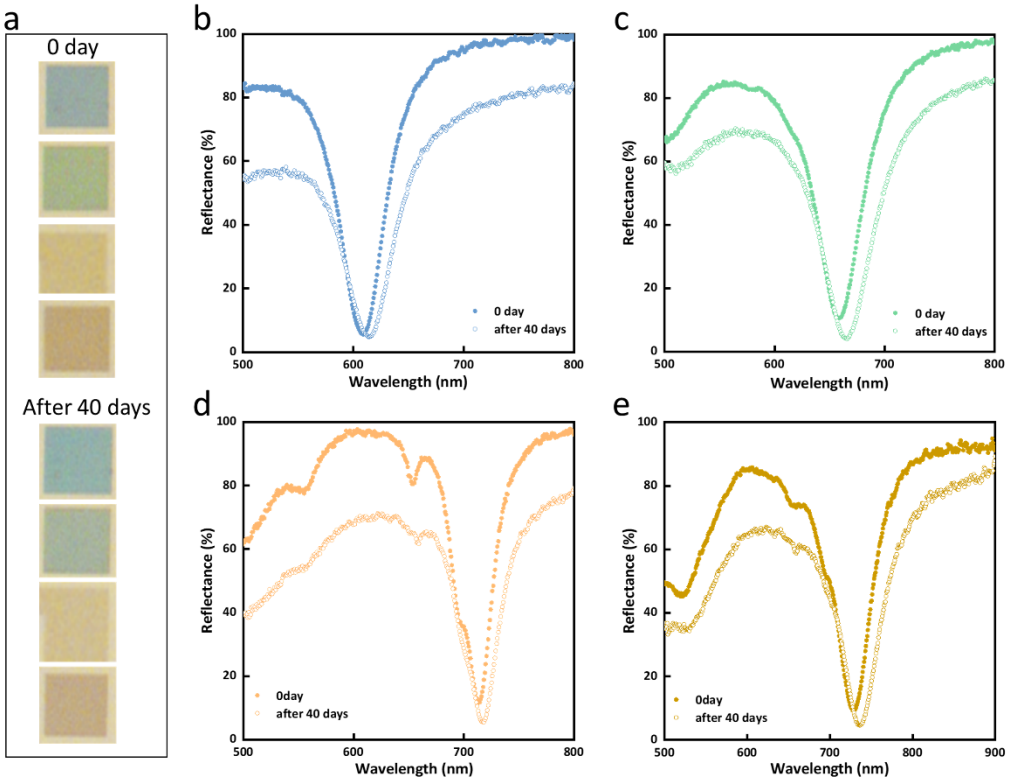

Supplementary Fig. S8. Durability of sodium plasmonic colors. (a) Optical images of the same sodium palette upon fabrication (Day 0) and after 40 days show a good capacity for color retention. (b), (c), (d) and (e) show the reflectance spectra comparison of the sodium palette upon fabrication (Day 0) and after 40 days.

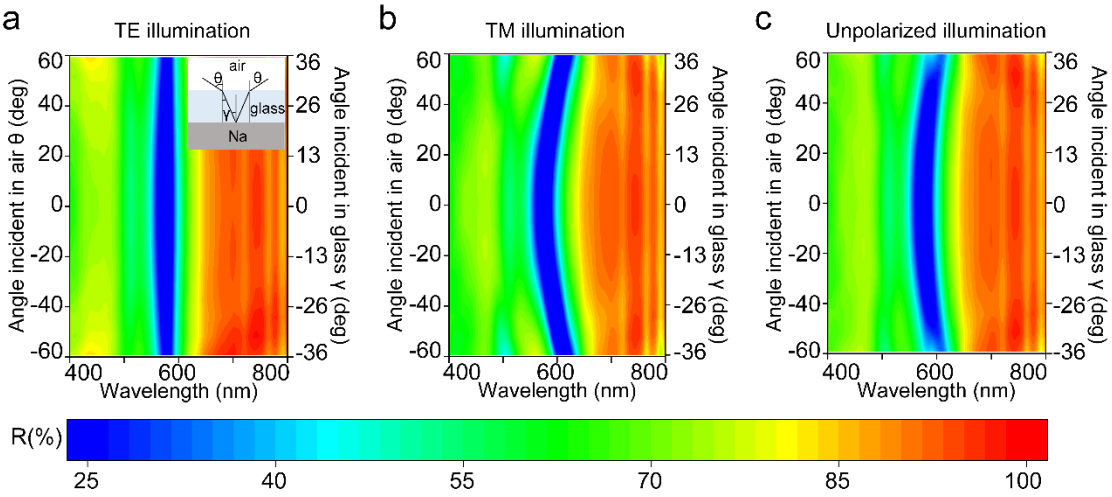

Supplementary Fig. S9. Simulated angular spectra of Na nanorods of p = 210 nm d = 160 nm h = 30 nm for TE, TM polarization and no polarization, respectively.

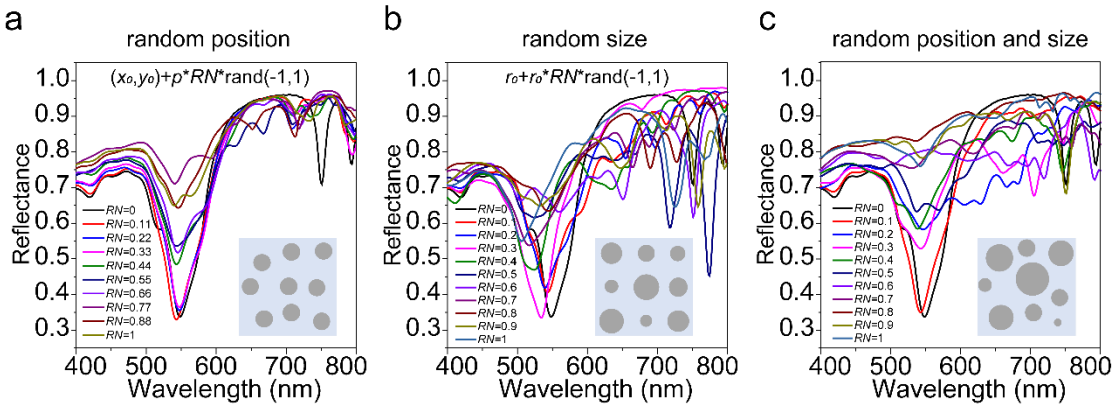

Supplementary Fig. S10. (a) Simulation results depicting the impact of positional randomness (*RN*) degree. (b) Simulation results depicting the impact of size randomness (*RN*) degree. (c) Simulation results depicting the impact of both positional and size randomness (*RN*) degrees. The simulated unit cell spans 630 nm in both the x and y directions, with periodic boundary conditions. Within this cell, 3×3 Na nanorods are positioned with radii defined as $r = r_0 + r_0*RN*\text{rand}(-1,1)$. Each nanorod is offset from the periodic Na nanorod positions (p = 210 nm, d = 120 nm, h = 30 nm) by $p*RN*\text{rand}(-1,1)$ along both x and y axes, where (x, y) coordinates are defined by $x=x_0+p*RN*\text{rand}(-1,1)$ and $y=y_0+p*RN*\text{rand}(-1,1)$). Here, the randomness factor (*RN*) is a value between 0 and 1.

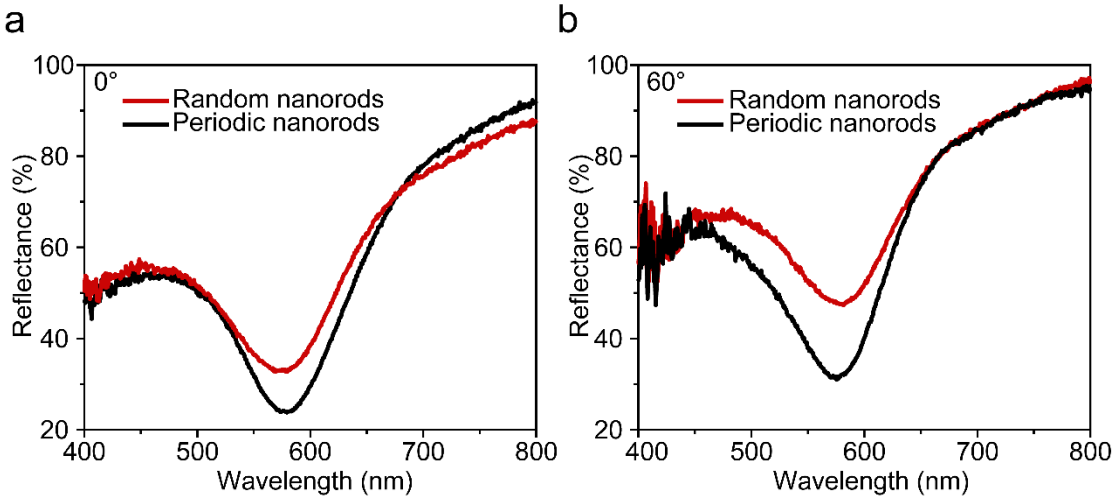

Supplementary Fig. S11. Experimental reflection spectra of random and periodic nanorods under the incidence angle of 0° (a) and 60° (b).

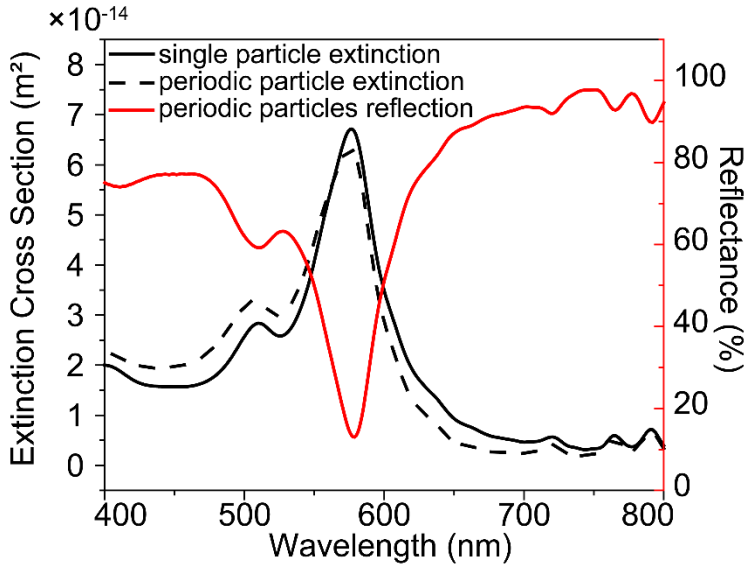

Supplementary Fig. S12. Simulated reflection spectrum of Na nanorods with *p*=210 nm, *d*=160 nm and *h*=30 nm and corresponding extinction cross-section spectra of single and periodic Na nanorod, exhibiting that the dominant LSPR mode of the Na nanorods.

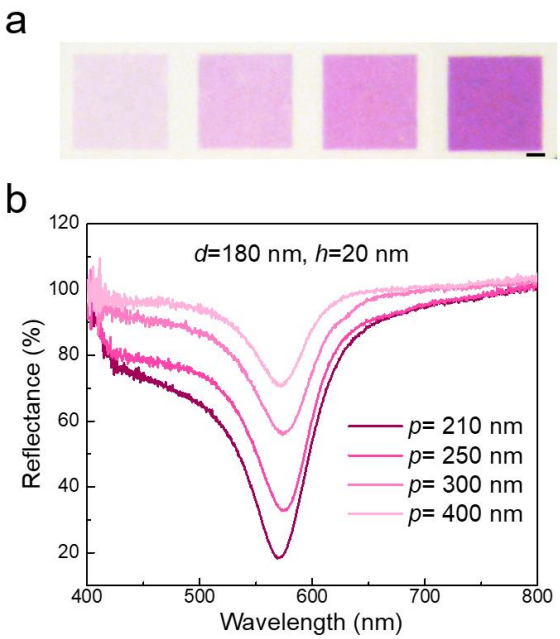

Supplementary Fig. S13. Microscope images (a) and reflectance spectra of the Na nanorods patterns (d=180 nm, h=20 nm) with different spatial densities (p=400 nm, 300 nm, 250 nm, 210 nm). The scale bar in (a) is 10 μm. The optical performance of periodic Na nanorods shows a clear trend: optical contrast significantly improves as spatial density increases (period decreases) from left to right, keeping the same resonance location.

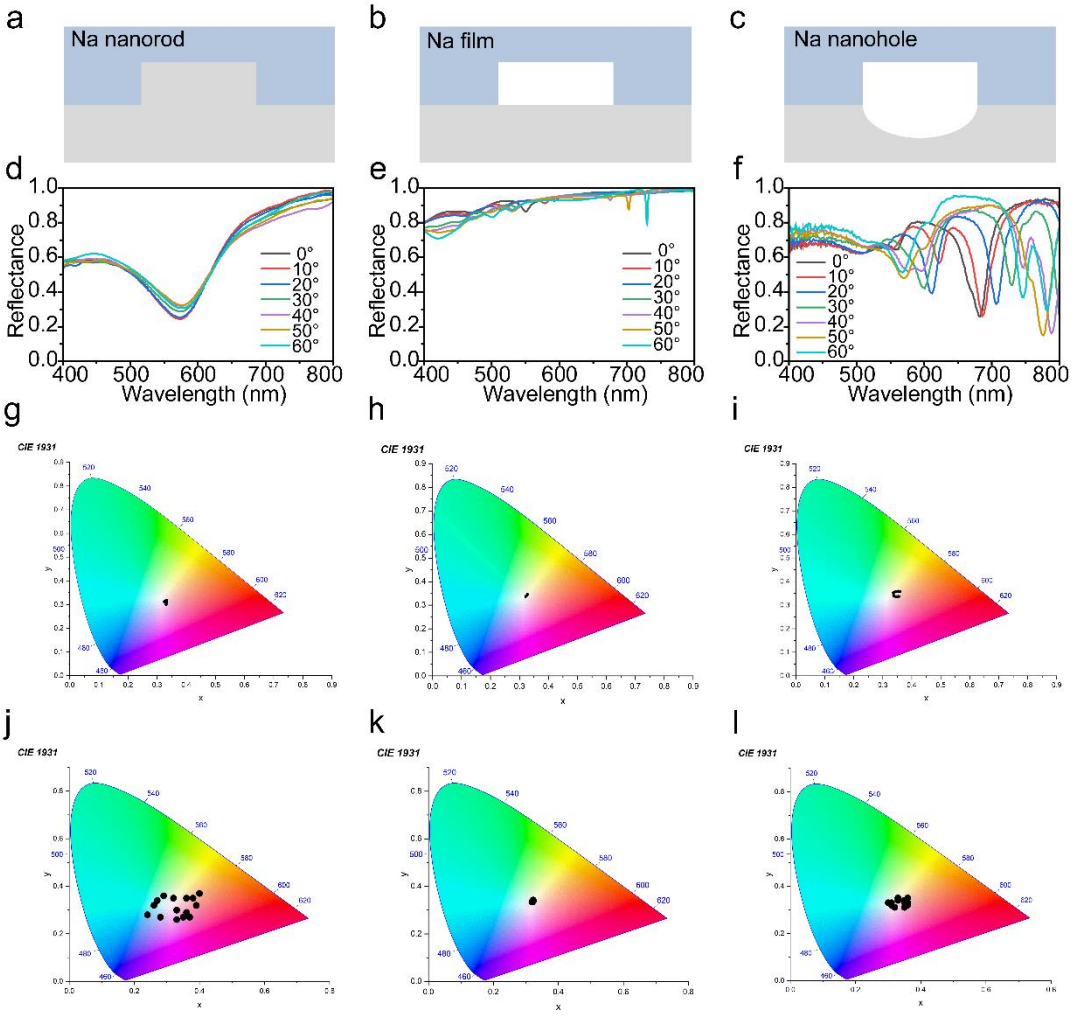

Supplementary Fig. S14. (a-c) The three different structure configurations schematics: Na nanorod (a), Na film (b) and Na nanohole (c). (d-f) Angular resolved reflectance spectra comparison of three different configurations: Na nanorod (p = 210 nm, d = 160 nm, h = 30 nm) (d), Na film (p = 300 nm, d = 170 nm, h = 50 nm) (e) and Na nanohole (p = 530 nm, d = 290 nm, h = 70 nm) (f). Note that the spectra of Na nanorod and Na nanohole configuration are experiment data, but the spectra of Na film configuration are simulation data. (g-i) The angle-resolved color gamut of Na nanorod arrays (g), Na film arrays (h) and Na nanohole arrays (i) under TM polarized illumination with varied incident angle from 0°-60°. (j-l) The color space of Na nanorod arrays (j), Na film arrays (k) and Na nanohole arrays (l) with various structure parameters.

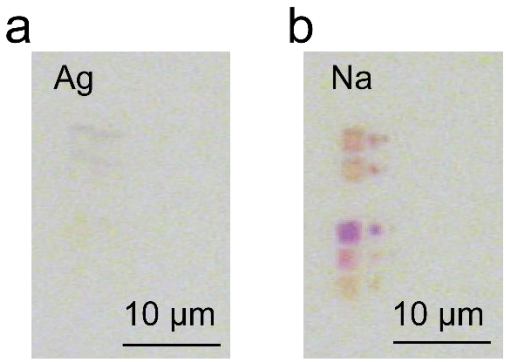

Supplementary Fig. S15. The bright field optical image of Ag based plasmonic color generation array (a) and Na based plasmonic color generation array (b) with p = 200 nm, d = 20-100 nm, h = 20 nm. It's obvious that the Ag arrays are colorless and Na arrays are colorful.

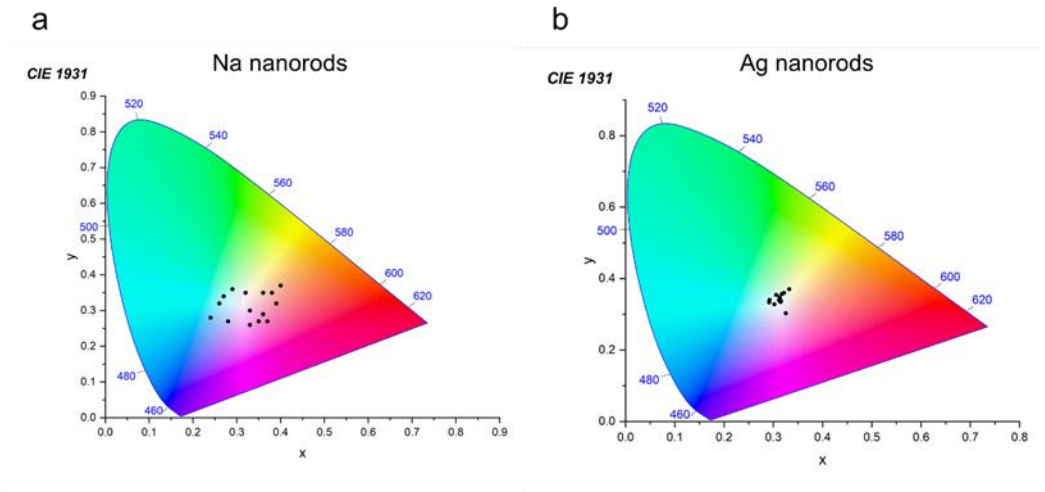

Supplementary Fig. S16. The color gamut of the Na nanorods based metasurface (a) and Ag nanorods based metasurface in experiments.

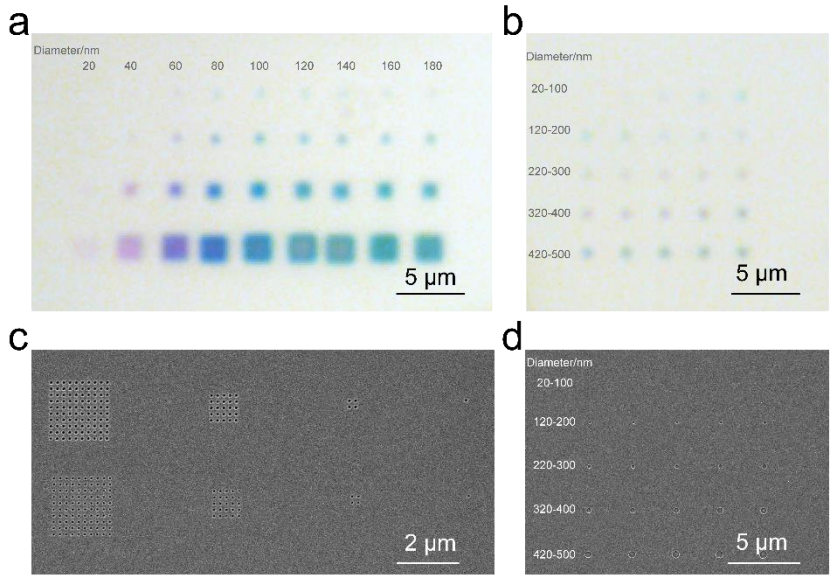

Supplementary Fig. S17. (a) The bright field optical image of fabricated plasmonic color pixels with 1×1, 2×2, 5×5, 10×10 periodic Na nanorod arrays of p = 200 nm, d = 20-180 nm, h = 50 nm. (b) The bright field optical image of a single Na nanorod with d varying from 20 nm to 500 nm, h = 50 nm. (c) The top-view SEM image of the substrate pattern of periodic Na nanorod arrays with p = 200 nm, d = 60, 80 nm, h = 50 nm in (a). (d) The top-view SEM image of the substrate pattern of single SNR in (b). It's distinct that the minimal pixel can be as small as a 60 nm single Na nanorod.

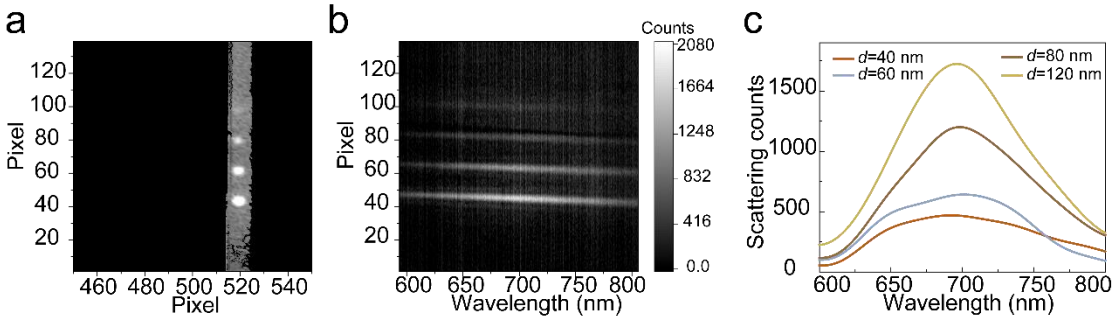

Supplementary Fig. S18. (a) The dark field optical image of single Na nanorod with *d* varying from 20 nm to 100 nm, *h* = 50 nm. (b) The dark field scattering experiment result of single Na nanorod with *d* varying from 20 nm to 100 nm, *h* = 50 nm. (c) The obvious experimental scattering spectra of single particles with *d* varying from 40 nm to 100 nm, *h* = 50 nm.

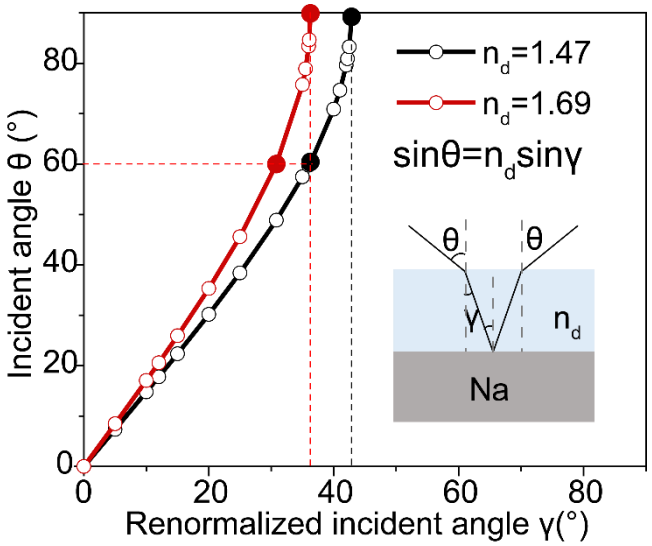

Supplementary Fig. S19. The incident-angle renormalization effect induced by the glass superstrate with a relatively high refractive index n_d.

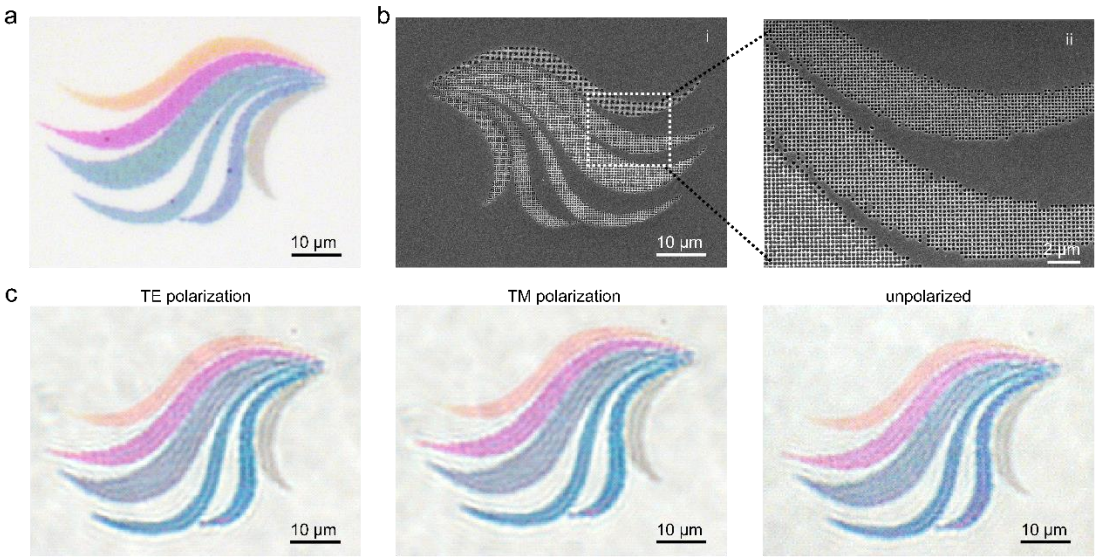

Supplementary Fig. S20. (a) The bright field optical microscope micrograph of the plasmonic painting of colorful strips at Kohler illumination. (b) The top-view SEM images of the painting of colorful strips. The scale bar of SEM is 10 μm (i) and 2 μm (ii). (c) The bright field optical microscope micrograph of the plasmonic painting of colorful strips under 0° incident illumination with different polarization.

Supplementary Table S1. Performance comparison of angle tolerant optical devices works.

Structure Design	Mechanism	Structure complexity	Precise manufacturability	Polarization insensitivity	Insensitive Angle	Pixel Size	Contrast ΔR	Reference
MIM Al-Al_2O_3-Al[2]	gap surface plasmon	3 layers (1+2+6)	*/	yes	70°	/	60-80%	*Proc Natl Acad Sci USA* 117, 13350-13358 (2020)
MIM Ag-SiO_2-Ag[3]	magnetic dipole resonance	3 layers (1+2+4)	1/7	yes	70°	300 nm	80-85%	*Sci Rep* 5, 11045 (2015)
Multilayer[4]	interference	3 layers (2*3)	1/6	yes	80°	2.5 μm	20-30%	*Nat Commun* 14, 565 (2023)
Multilayer[5]	interference	4 layers (2*4)	1/8	yes	50°	/	50-80%	*Sci Rep* 5, 9285 (2015)
Multilayer[6]	interference	7 layers (2*7)	1/14	yes	60°	/	80-90%	*Opt Lett* 46, 5161-5164 (2021)
Multilayer[7]	interference	4 layers (2*4)	1/8	yes	/	100 nm	60-85%	*Nat Nanotechnol* 16, 795-801 (2021)
Random Ag NDs[8]	random particle plasmon	1 layer (5)	1/5	yes	60°	/	30-50%	*Opt Lett* 40, 4979-4982 (2015)
Si_3N_4 metasurface[9]	transmission metasurface	1 layer (6)	1/6	/	20°	>10 μm	/	*Optica* 9, 431-437 (2022)
Si_3N_4 metasurface[10]	transmission metasurface	1 layer (6)	1/6	/	30°	2 μm	/	*Nat Commun* 13, 3288 (2022)
Ag metasurface[11]	reflective metasurface	1 layer (6)	1/6	no	15°-45°	n μm	15-65%	*Nat Nanotechnol* 18, 71–78 (2023)
Multilayer[12]	F-P cavity	4 layers (2*4)	1/8	yes	/	5 μm	50-60%	*Adv Photonics Nexus* 1, 026002 (2022)
Li NPs[13]	reflective metasurface	3 layers (1+2+4)	1/7	yes	/	1 μm	20-50%	*Natl Sci Rev* 10, nwac120 (2023)
Na nanorods	**reflective metasurface**	**1 layer (4) (#3)**	**1/4 (#1/3)**	**yes**	**64° (※90°)**	**60 nm**	**80-90% (★)**	**This work**

*Self-assembly nanoparticles can't be precisely manufactured.

p (period) has little effect. ※ In theory. ★ for optimized Na nanorods at high density.

Note: The "Precise manufacturability" is defined by the reciprocal of precise structure complexity, but self-assembly nanoparticles by e-beam evaporation are heterogeneous and can't be precisely controlled, thus are not included in the comparison. The structure complexity is defined by the total parameters of the nanostructure ($\sum_1^{layers} parameters$). The *parameters* of each layer is defined as following: *parameters*=1 for a single layer; *parameters*=2 for a single layer with a fixed thickness; *parameters*=3 for a layer containing nanorods with fixed diameter and height; *parameters*=4 for a layer containing nanostructures with fixed period, diameter and height; *parameters*=5 for a layer containing randomly positioned nanostructures with fixed diameter, height, gap range and position randomness; *parameters*=6 for a layer containing randomly sized and positioned nanostructures with fixed height, diameter range, gap range, size randomness and positioned randomness or a layer containing rectangular nanostructures with fixed height, length, width, period along length and

period along width or a layer containing square nanostructures with fixed height, length range, gap range, different lengths variety and position variety.